KLL dielectronic recombination resonant strengths of He-like up to O-like xenon ions

K. Yao,[1,2] Z. Geng,[1,2] J. Xiao,[1,2] Y. Yang,[1,2] C. Chen,[1,2] Y. Fu,[1,2] D. Lu,[1,2] R. Hutton,[1,2] and Y. Zou[1,2,*]

[1]*The Key Laboratory of Applied Ion Beam Physics, Ministry of Education, People's Republic of China*

[2]*Shanghai EBIT Laboratory, Institute of Modern Physics, Fudan University, Shanghai, People's Republic of China*

(Received 9 December 2009; published 18 February 2010)

In this work, the *KLL* dielectronic recombination (DR) resonant strengths of He- through to O-like Xe ions were studied, both through experiment and calculation. The experiments were done using a fast electron beam-energy scanning technique at the Shanghai electron beam ion trap. The calculations were done by using the flexible atomic code (FAC), in which the relativistic configuration interaction (RCI) method was employed. For the total resonant strengths, the present experimental and theoretical results for He-, Be-, B-, C-, N-, and O-like Xe ions agree within experimental uncertainties (about 9%). But the experimental result for Li-like Xe is 14% higher than the calculation. The present FAC calculations of the total DR strengths were compared with the available previous calculations, using RCI or multiconfiguration Dirac-Fock (MCDF) methods, and the agreement was very good. In this work, some intermediate-state resolved *KLL* DR strengths were also obtained and compared with theoretical results, and more discrepancies were revealed.

DOI: 10.1103/PhysRevA.81.022714 PACS number(s): 34.80.Lx, 31.15.V−, 52.20.Hv, 52.20.Fs

I. INTRODUCTION

Dielectronic recombination (DR) is an important process in high-temperature plasmas [1–8]. It affects the charge state balance and energy-level populations as well as the plasma temperature. Resolvable satellite lines caused by DR are often used for electron temperature determinations in plasma diagnostics. However, unresolvable satellite lines disturb the determination of line shapes, line intensity, and line position, consequently corrupting the determination of temperature, density, and ion movement in plasmas. Therefore, whether the influence of DR be good or bad to the plasmas, DR plays an important role, and its occurrence strength is vital for accurate modeling of high-temperature plasmas. DR studies are also important for testing atomic structure and atomic collision theories since such resonances carry information on quantum electrodynamics, relativistic effects, electron correlations, and so on.

DR is a resonant process, in which a free electron is captured by an ion, at the same time a bound electron in the ion is promoted, forming a multiply excited intermediate state situated above the autoionization threshold. The process is finally completed by stabilization through emitting one or more photons, so as to reduce the ion energy to below its ionization limit. It is generally labeled using an inverse Auger process notation. For instance, a process in which an electron is captured, whereas a bound electron is excited from the K shell, results in an autoionization state where one of the two active electrons is in the L shell, and the other is in an n shell (n can be L, M, N, O, etc.). This is labeled as a KLn DR process. A *KLL* DR from the ground state of a He-like ion can be described as follows:

$$1s^2 + e^- \rightarrow 1s2l2l' \rightarrow 1s^2 2l' + h\nu, \qquad (1)$$

where l and l' denote angular momentum quantum numbers.

The DR process was first studied in a theoretical work by Massey and Bates [9] in 1942. However, the first experimental study of DR resonant strengths had to wait for 41 years and was performed using crossed-beam methods [3]. Utilization of ion storage rings and electron beam ion traps and sources (EBIT and EBIS) gives opportunities for a wide range of experimental studies of DR processes. DR studies at storage rings are mostly focused on experiments with low electron-ion interaction energies, such as resonances involving a $\Delta n = 0$ excitation in a heavy few electron ions, or involving a $\Delta n > 0$ excitation in light ions [10–17]. Recently a new operational scheme at the GSI ESR storage ring was tested, and using this, it was possible to study *KLL* DR for H-like uranium [18]. In high-Z few electron ions, higher electron ion collision energies are needed for $\Delta n > 0$ DR processes, especially for those involving a K electron excitation. EBIT and EBIS are commonly employed in these cases. By using EBIT/EBIS, DR of He-like ions was studied for many species: argon [19–22], iron [23,24], germanium [25], titanium [26], nickel [27], molybdenum, and barium [28]. DR for other open L-shell ions has been studied (e.g., for holmium and bismuth [29], krypton [30], iodine [29,31], and xenon [32,33]). Also the iso-electronic sequences of H-like [34], F-like [35], and Ne-like ions [36,37] have been studied.

For the *KLL* DR processes in open, but not empty, L-shell ions, the intermediate states will have more than two L-shell electrons. This leads to extensive correlation effects, which introduce more challenges for a good theoretical description. Experimental studies with a good level of precision are very much required to test the theories. In our previous work, resonant energies and resonance strengths for *KLL* DR of open L-shell Xe ions were studied by measuring the stabilizing X ray while scanning the electron beam energy in a steady-state mode [32,33]. We could determine the resonant energies for He-like up to O-like Xe ions at an average accuracy level of 0.03% [33], with the help of a homemade precise and highly stable high-voltage divider [38]. But for the resonance strength studies [33], we could only make measurements for Be-, B-, and C-like Xe ions, and even then with uncertainties between 15% and 20%. This is mainly because in the steady-state mode we have less control over the charge state distribution of the

*Zouym@fudan.edu.cn

ions. In fact the charge state balance changes when scanning through a DR resonance in the steady-state mode, as the ions have time to recombine in a significant number. Hence, we could only measure the resonance strengths for Be-, B-, and C-like Xe ions. The change in the charge state distribution when scanning through a resonance makes data analysis extremely complicated. This in turn led to substantial contributions to the high uncertainties in our previous resonance strength studies. In the present work, by using a fast electron energy scanning scheme, we studied the *KLL* DR resonance strengths for all the possible charge states of Xe ions with open *L* shell (from He-like up to O-like), at a significantly improved accuracy level. We also made fully relativistic calculations and compared the results with our experimental results.

II. EXPERIMENT

In an EBIT, an electron beam is emitted by an electron gun and accelerated by the high voltage applied between the electron gun and the central drift tube. At the same time the electron beam is compressed to a diameter below 100 μm by a few Tesla magnetic field. Neutral atoms or low charge ions are injected into the central drift tube, where they are ionized and trapped. Radial trapping is provided by the combined effects of the electron beam space charge and the magnetic field. The ions are axially trapped by a potential well formed by a bias voltage that is applied to the drift tubes. Then, in the central drift tube, which is the trap region in an EBIT, a special plasma is formed with almost single, but tunable energy electrons. The charge state balance of this plasma depends mainly on the electron energy and density. This makes an EBIT unique in disentanglement studies of electron collision processes in plasmas.

The experiments in the work presented here were performed at the Shanghai EBIT [39,40]. The experimental setup was similar to that described in our previous work [32] except for the timing scheme for scanning the electron beam energy (see Fig. 1). The timing scheme employed here started with 4 s charge breeding time (cooking time) at the electron beam energy of 23.0 keV, to obtain the desired charge state distribution. The beam energy was then ramped linearly down through the *KLL* DR resonances to 19.8 keV and back up in 25 ms. The beam energy was then kept at 23.0 keV for another 75 ms before the next ramping in order to maintain the charge state distribution. After 80 ramping-maintaining circles, the trap was dumped to prevent accumulation of other heavy ions, such as tungsten and barium, which could be sputtered from the cathode of the electron gun and make their way into the trap. The trap was then refilled with fresh ions and another cooking-ramping-maintaining circle was started. During the experiments, xenon gas was introduced continuously into the

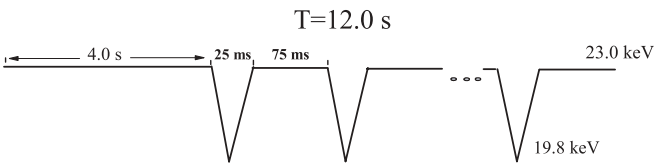

FIG. 1. Time sequence for the electron beam energy in the present experiments at Shanghai EBIT.

TABLE I. EBIT operating parameters in this work. Different trap depth and xenon gas injection pressure were used in experiments A and B, while the others were fixed.

Parameter	Value
Beam current	70 mA
Beam radius	35 μm
Magnetic field	3 T
Beam energy	19.8−23.0 keV
Energy sweep rate	0.256 eV/μs
Trapping time	12.0 s
Trap depth (Expt. A)	20 V
Gas pressure (Expt. A)	5.0×10^{-9} torr
Trap depth (Expt. B)	200 V
Gas pressure (Expt. B)	1.0×10^{-8} torr

drift tube region of the EBIT. The EBIT operation parameters for the experiments are listed in Table I. It was not possible to produce all charge states from He-like to O-like Xe in one experiment. Hence, we performed two experiments (A and B) where the trap depths and gas injection pressures were changed. All other EBIT parameters were kept fixed. The conditions used in experiment A favored higher charge state production. Each run contains 10 measurements.

X rays emitted by the trapped ions were observed by a high purity germanium detector mounted perpendicular to the electron beam. The X-ray energy, electron beam energy, and the time were all recorded simultaneously. Figures 2 and 3 show examples of the kind of scatter plots recorded in experiments A and B, respectively. The bright dots represent the *KLL* DR events of the xenon ions.

III. DATA ANALYSIS

The resonance strength for an isolated DR resonance from an initial state *i* through a doubly excited state *d* to a final state

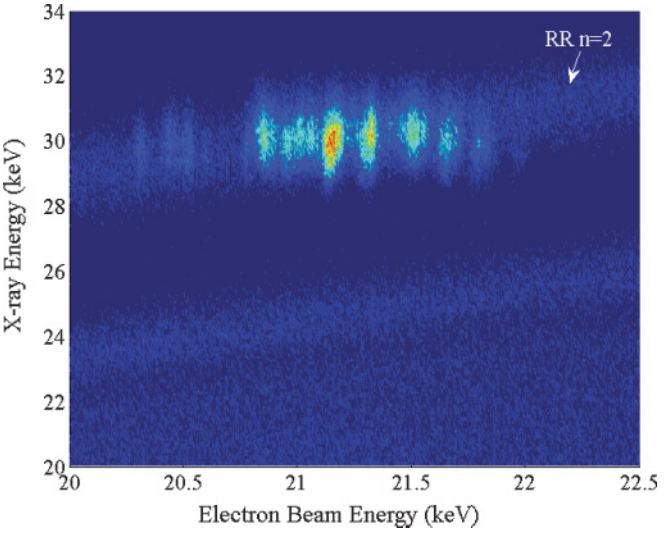

FIG. 2. (Color online) A scatter plot from experiment A, the *x* axis for electron energy, and the *y* axis for X-ray energy.

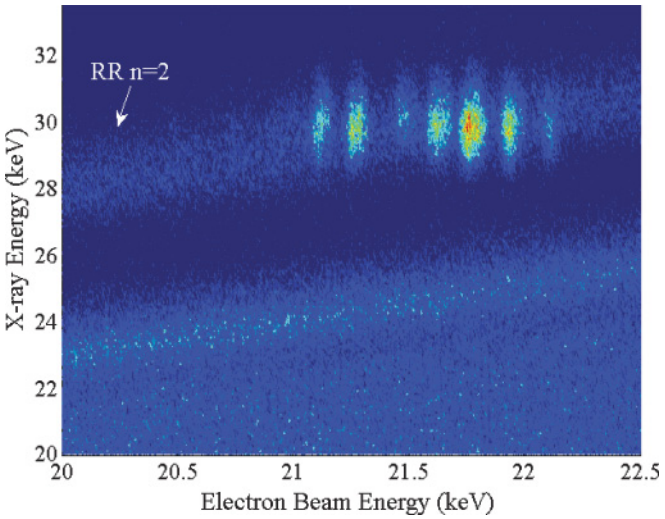

FIG. 3. (Color online) A scatter plot from experiment B, the x axis for electron energy, and the y axis for X-ray energy.

f can be expressed as

$$S_{idf} = \int_0^\infty \sigma_{idf}(E)dE = \frac{g_d}{2g_i}\frac{\pi^2\hbar^3}{m_e E_{\rm res}}\frac{A_r(d\to f)A_a(d\to i)}{\sum A_r + \sum A_a}, \quad (2)$$

where g_i and g_d are statistic weights of the initial state and the intermediate state of the DR process, respectively, A_r is the radiative transition rate, A_a is the autoionization rate, and $E_{\rm res}$ is the resonant energy. The summation is over all the possible autoionization and radiative decay channels from the intermediate state. The natural width of the cross section has a Lorentz profile [41]:

$$\sigma(E) = \frac{S}{\pi}\frac{\Gamma/2}{(E-E_{\rm res})^2+(\Gamma/2)^2}, \quad (3)$$

where E is the incident electron energy and Γ is the total energy width of the doubly excited state.

In an EBIT, the electron beam has an energy spread which is well accepted to be described by a Gaussian function [23,25,27]. So the theoretical cross sections have to be convoluted with the electron energy distribution for comparison with the experimental results. This convolution results in a Voigt profile:

$$V(E) = \frac{2\ln 2}{\pi\sqrt{\pi}}\frac{\Gamma}{w^2}\int_{-\infty}^{\infty}\frac{\exp(-t^2)}{(x-t)^2+a^2}dt, \quad (4)$$

where $a = \sqrt{\ln 2}\Gamma/w$, $x = 2\sqrt{\ln 2}(E-E_{\rm res})/w$, and w is the FWHM (full width at half maximum) of the electron beam energy distribution, typically several tens of eV in an EBIT.

Another important fact that has to be accounted for is the angular distribution of the stabilization radiation of the DR processes. The reason is that the collisions involve a unidirectional electron beam, which will lead to an uneven population of the magnetic sublevels. The consequent radiation from relaxation of the excited state will then have some degree of polarization [42–46]. Because in a DR process, the stabilization radiation must compete with autoionization from the intermediate state d, and the latter is a very fast process, the dominating stabilization radiation is, in most cases, through electric dipole transitions. In this work, we observed the radiation at 90° to the electron beam. For electric dipole transitions, the angular correction factor can be expressed as follows:

$$W_{df}(\pi/2) = \frac{3}{3-P}, \quad (5)$$

where P is the degree of linear polarization.

In the data analysis presented here, all the measured scatter plots were cut along the $n=2$ radiative recombination (RR) and then projected onto the electron beam energy axis to obtain the excitation functions for DR plus RR for both experiments A and B. To get better statistics, all ten excitation functions from experiments A and B were added together, respectively, as shown in Figs. 4 and 5. In both figures, the continuous background is mostly from $n=2$ RR, while the resonant peaks correspond to the *KLL* DR events. The excitation function can

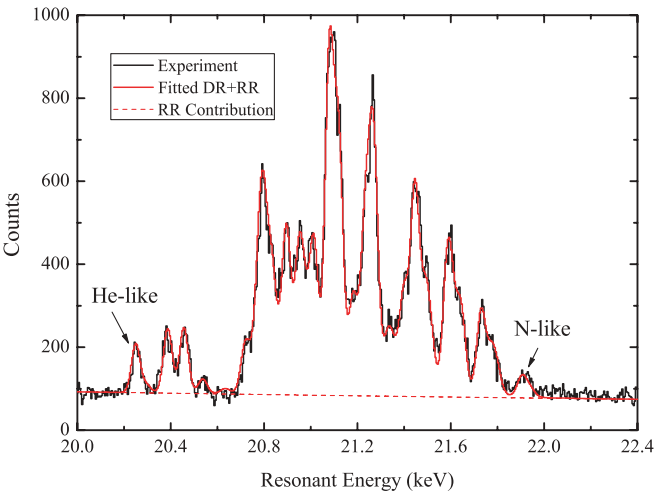

FIG. 4. (Color online) The excitation function from experiement A. Solid line showing the Fitting result. Dashed line showing the contribution of the $n=2$ RR.

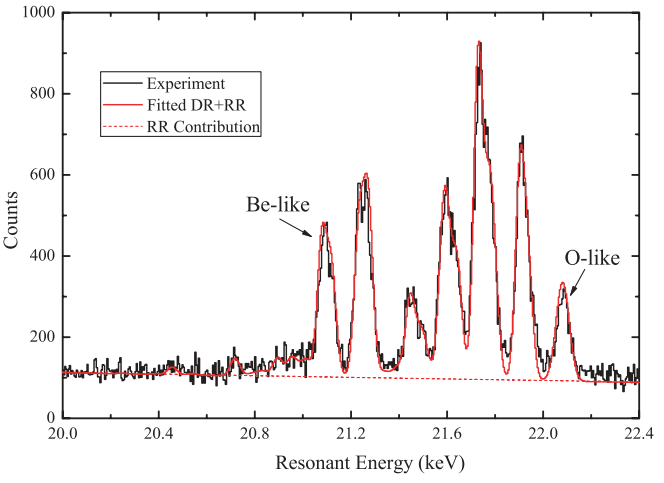

FIG. 5. (Color online) The excitation function from experiment B. Solid line showing the Fitting result. Dashed line showing the contribution of the $n=2$ RR.

then be expressed as:

$$I(E) = D(E)\sum_q f_q \left[\frac{d\sigma_{RR}(q,E)}{d\Omega} + K_q \sum_{d,f} \frac{S_{qdf} W_{qdf}(\pi/2)}{4\pi} V(E)\right], \quad (6)$$

where $D(E)$ is a detection efficiency coefficient containing the detector efficiency, electron density, ion density, detection time, overlapping area, and so on, f_q is the ion abundance of charge state q, $d\sigma_{RR}(q,E)/d\Omega$ is the differential cross section of $n = 2$ RR at 90°, S_{qdf} is the DR resonant strength from the ground state of the ions of charge state q through intermediate state d to final state f, W_{qdf} is the corresponding angular correction factor, and $V(E)$ is the Voigt distribution of the DR resonance profile discussed above. K_q is a factor used for correcting theoretical resonance strengths and only used in the preliminary data analysis.

We made preliminary fits to the experimental data using the above expression (6). In this fit, the detection efficiency coefficient $D(E)$, the ion abundance f_q, the resonant strength correction factor K_q, and the Gaussian width w of the electron energy in the Voigt distribution were free parameters. Throughout the data analysis, the resonance energies used were those obtained in our previous experiment [33]. For the energies which were not covered by the above-mentioned experiment, we employed the theoretical results calculated using the flexible atomic code (FAC), developed by Gu [47]. The same code was used in calculating the RR differential cross sections, the resonant strengths, and the energy widths of the intermediatate states Γ of the DR processes, and the angular correction factor W_{df}. In the preliminary data fits, theoretical obtained DR strengths were used to get the detection efficiency coefficient $D(E)$, the ion abundance f_q, the resonant strength correcting factor K_q, as well as the Gaussian width w of the electron energy in the Voigt distribution. The values for these quantities are listed in Table II. We then fixed these parameters and released the DR resonant strengths as the fitting parameters. This gave us the final results for the DR resonant strengths. For the final fitting, we removed the resonant strength correction factor K_q from the above expression. The red solid lines in Figs. 4 and 5 show the fitting results; the agreement between the fitting and the experiments is excellent.

TABLE II. The fitted ion abundance f_q (%), resonant strength correction factor K_q, and the Gaussian width of the electron energy w (eV).

	He	Li	Be	B	C	N	O	F
Expt. A	9.5	19.0	25.2	24.7	14.1	7.5	0	0
Expt. B	0	0.7	3.6	10.4	18.4	25.4	22.9	18.6
K_q	0.972	1.094	1.020	1.025	0.998	1.035	1.057	–
$D(E)$	Expt. A $= 2.56 \times 10^{25}$				Expt. B $= 7.72 \times 10^{25}$			
w	42.8							

Using the FAC code, we calculated the RR differential cross sections for the electron energies from 20.0 to 23.0 keV, with steps of 100 eV. For electron energies between the 100 eV steps, an interpolation scheme was used to obtain the cross sections. The interpolated results were then checked by additional careful FAC calculation to ensure a deviation within 0.05%. For the *KLL* DR calculations, $1s^2(2l)^p$, $1s^2(2l)^{p-1}nl'$, and $1s(2l)^{p+1}$ configurations were included for the initial states, $1s(2l)^{p+2}$ and $1s(2l)^{p+1}nl'$ for the intermediate states, and $1s^2(2l)^{p+1}$, $1s^2(2l)^p nl'$, and $1s(2l)^{p+2}$ for the final states. Here p is the number of electrons in the L shell, for the charge states from He-like to O-like, it is, respectively, from zero up to six. For He-like ions, the initial state calculation included $1s^2$ and $1snl$ configurations. In the calculations, the configurations of principle quantum number $n = 3, 4, 5$ and all their possible angular momentum states, l, are included. In Table III, we list the calculated resonant energies, resonant strengths, and the corresponding energy widths of the intermediate states for He-like up to O-like Xe ions from this work. Also shown are the experimental resonant energies from [33] and the theoretical resonance strengths from [48–50]. The resonant process for each intermediate state is labeled by its initial charge state and a number. From this table we can see that the calculated resonant energies in this work agree very well with the experimental results from [33]. It is also worth noting that the numbers in the last column, the theoretical *KLL* DR strengths of He-like xenon, were obtained using the resonant energies calculated in this work and the autoionization and radiative rates from Nilsen's work [48]. Because of the excellent agreement of the present energy calculations with the experiments in [33], and generally rather accurate energy calculation, we consider the reliability of the obtained DR resonant strengths should depend mainly on the rate calculations in Nilsen's data [48].

Table IV lists the labels of the final states of the stabilizations from the *KLL* DR resonances of the He- through to N-like Xe ions involved in this work. In Tables V–X, we listed the calculated angular correction factors W_{qdf} for the main DR processes of He-like up to N-like Xe ions. The factors are 1 for all the O-like *KLL* DR resonance stabilization transitions.

In our data analysis, we assumed the charge state distribution remained constant during the measurements. In fact, it must change as the electron beam energy is scanned across DR resonances. For example, a fraction of the He-like Xe ions become Li-like as the electron energy is swept over a DR resonance. This can be expressed as [28]

$$\frac{\Delta N_{\rm He}}{N_{\rm He}} = -\left\langle \frac{j_e}{e} \right\rangle S_{\rm He} \frac{dt}{dE}, \quad (7)$$

For the ions of lower charge state q, compensation from the next higher charge state should be considered:

$$\frac{\Delta N_q}{N_q} = -\left\langle \frac{j_e}{e} \right\rangle \frac{dt}{dE}\left(S_q - \frac{N_{q+1}}{N_q} S_{q+1}\right), \quad (8)$$

where $\langle j_e \rangle$ is the effective current density and dE/dt is the energy sweep rate.

Using theoretical resonance strengths, we could estimate for He-like Xe ions that the abundance change during the energy scanning was less than 1.5% under the experiment

TABLE III. The calculated resonant energies, resonant strengths, and the energy widths, Γ (eV), of the intermediate doubly excited states of the *KLL* DR of He-like up to O-like Xe ions of this work, together with the experimental resonant energies from [33] and the theoretical resonance strengths from [48–50].

		E_{res} (eV)			S (10^{-20} cm^2 eV)	
Label	State	Theor.	Expt. [32]	Γ (eV)	Theor.	Theor.
He1	$[1s2s^2]_{1/2}$	20246	20244(9)	0.29	2.57	2.59[a]
He2	$[(1s2s)_1 2p_{1/2}]_{3/2}$	20293		1.74	0.56	0.54[a]
He3	$[(1s2s)_0 2p_{1/2}]_{1/2}$	20379	20385(8)	1.82	3.24	3.27[a]
He4	$[(1s2s)_1 2p_{3/2}]_{3/2}$	20712		4.25	0.37	0.26[a]
He5	$[(1s2s)_1 2p_{3/2}]_{1/2}$	20749		4.33	1.12	1.07[a]
He6	$[(1s2s)_0 2p_{3/2}]_{3/2}$	20776		0.72	4.57	4.71[a]
He7	$[(1s2p_{1/2})_1 2p_{3/2}]_{5/2}$	20796		2.03	7.29	7.24[a]
He8	$[(1s2p_{1/2})_0 2p_{3/2}]_{3/2}$	20833		5.52	6.20	5.53[a]
He9	$[1s(2p_{3/2})^2_2]_{5/2}$	21179		1.34	4.35	4.48[a]
He10	$[1s(2p_{3/2})^2_2]_{3/2}$	21221		6.91	2.35	2.20[a]
He11	$[1s(2p_{3/2})^2_0]_{1/2}$	21246		3.50	0.77	0.78[a]
Li1	$[1s2s^2 2p_{1/2}]_1$	20456	20454(5)	2.06	1.43	
Li2	$[(1s2s)_1(2p_{1/2})^2]_1$	20540	20535(6)	2.45	0.41	
Li3	$[1s2s^2 2p_{3/2}]_2$	20827		0.26	0.86	
Li4	$[1s2s^2 2p_{3/2}]_1$	20862		4.86	0.43	
Li5	$[((1s2s)_1 2p_{1/2})_{1/2} 2p_{3/2}]_2$	20865		0.57	0.21	
Li6	$[((1s2s)_1 2p_{1/2})_{3/2} 2p_{3/2}]_3$	20893		1.82	3.74	
Li7	$[((1s2s)_1 2p_{1/2})_{1/2} 2p_{3/2}]_1$	20928		6.19	0.47	
Li8	$[((1s2s)_1 2p_{1/2})_{3/2} 2p_{3/2}]_2$	20950		5.07	3.45	
Li9	$[((1s2s)_1 2p_{1/2})_{3/2} 2p_{3/2}]_1$	20977		6.04	1.82	
Li10	$[((1s2s)_0 2p_{1/2})_{1/2} 2p_{3/2}]_1$	21005		1.49	0.23	
Li11	$[((1s2s)_0 2p_{1/2})_{1/2} 2p_{3/2}]_2$	21012		3.19	3.07	
Li12	$[(1s2s)_1(2p_{3/2})^2_2]_3$	21263		1.52	2.84	
Li13	$[(1s2s)_1(2p_{3/2})^2_2]_2$	21329		5.90	1.51	
Li14	$[(1s2s)_1(2p_{3/2})^2_0]_1$	21355		3.54	0.68	
Li15	$[(1s2s)_1(2p_{3/2})^2_2]_1$	21381		7.06	0.63	
Li16	$[(1s2s)_0(2p_{3/2})^2_2]_2$	21395		1.97	1.45	
Be1	$[1s2s^2(2p_{1/2})^2]_{1/2}$	20715	20715(5)	2.99	0.91	0.95[b]
Be2	$[(1s2s^2 2p_{1/2})_1 2p_{3/2}]_{5/2}$	21076	21077(4)	2.18	6.10	5.82[b]
Be3	$[(1s2s^2 2p_{1/2})_0 2p_{3/2}]_{3/2}$	21112	21117(5)	5.55	5.54	5.05[b]
Be4	$[1s2s^2(2p_{3/2})^2_2]_{5/2}$	21444		1.56	3.59	3.86[b]
Be5	$[1s2s^2(2p_{3/2})^2_2]_{3/2}$	21485		6.91	2.16	1.47[b]
Be6	$[1s2s^2(2p_{3/2})^2_0]_{1/2}$	21510		2.31	1.04	1.22[b]
B1	$[1s2s^2(2p_{1/2})^2 2p_{3/2}]_2$	21231	21231(4)	3.06	3.09	2.98[c]
B2	$[1s2s^2(2p_{1/2})^2 2p_{3/2}]_1$	21266	21270(5)	7.53	2.64	2.61[c]
B3	$[(1s2s^2 2p_{1/2})_1(2p_{3/2})^2_2]_2$	21577		2.55	1.59	1.78[c]
B4	$[(1s2s^2 2p_{1/2})_1(2p_{3/2})^2_2]_3$	21594		3.51	1.79	2.05[c]
B5	$[(1s2s^2 2p_{1/2})_1(2p_{3/2})^2_2]_1$	21615		8.72	0.76	0.54[c]
B6	$[(1s2s^2 2p_{1/2})_0(2p_{3/2})^2_2]_2$	21638		7.68	1.28	0.92[c]
B7	$[(1s2s^2 2p_{1/2})_1(2p_{3/2})^2_0]_1$	21643		5.58	0.71	0.83[c]
B8	$[(1s2s^2 2p_{1/2})_0(2p_{3/2})^2_0]_0$	21648		3.55	0.23	0.27[c]
C1	$[1s2s^2(2p_{1/2})^2(2p_{3/2})^2_2]_{5/2}$	21730	21728(5)	4.42	2.96	
C2	$[1s2s^2(2p_{1/2})^2(2p_{3/2})^2_2]_{3/2}$	21771	21772(6)	9.55	1.94	
C3	$[1s2s^2(2p_{1/2})^2(2p_{3/2})^2_0]_{1/2}$	21785	21796(10)	6.45	0.82	
N1	$[1s2s^2(2p_{1/2})^2(2p_{3/2})^3_{3/2}]_2$	21904	21902(4)	6.73	1.63	
N2	$[1s2s^2(2p_{1/2})^2(2p_{3/2})^3_{3/2}]_1$	21936	21933(4)	10.56	0.97	
O1	$[1s2s^2(2p_{1/2})^2(2p_{3/2})^4]_{1/2}$	22083	22082(4)	9.88	0.81	

[a]Reference [48].
[b]Reference [49].
[c]Reference [50].

condition listed in Table I. From the previous two expressions plus the fact that the total DR strength for He-like ions is larger than those of the other charge states concerned in this work, the abundance change of other charge states would not exceed 1.5%. So the assumption of a constant charge state distribution can be considered as fairly safe.

TABLE IV. Labels of the final states of the stabilizations in He-like to N-like *KLL* DR processes.

Index	State	Index	State
HeLi0	$[2s_{1/2}]_{1/2}$	BeB12	$[2p_{1/2}(2p_{3/2})^2_2]_{5/2}$
HeLi1	$[2p_{1/2}]_{1/2}$	BeB13	$[2p_{1/2}(2p_{3/2})^2_0]_{1/2}$
HeLi2	$[2p_{3/2}]_{3/2}$	BC0	$[2s^2(2p_{1/2})^2_0]_0$
LiBe0	$[2s^2]_0$	BC1	$[2s^22p_{1/2}2p_{3/2}]_1$
LiBe1	$[2s_{1/2}2p_{1/2}]_0$	BC2	$[2s^22p_{1/2}2p_{3/2}]_2$
LiBe2	$[2s_{1/2}2p_{1/2}]_1$	BC5	$[2s^2(2p_{3/2})^2_2]_2$
LiBe3	$[2p^2_{1/2}]_0$	BC6	$[2s^2(2p_{3/2})^2_0]_0$
LiBe4	$[2s_{1/2}2p_{3/2}]_2$	CN0	$[2s^2(2p_{1/2})^22p_{3/2}]_{3/2}$
LiBe5	$[2s_{1/2}2p_{3/2}]_1$	CN1	$[2s^22p_{1/2}(2p_{3/2})^2_2]_{3/2}$
LiBe6	$[2p_{1/2}2p_{3/2}]_1$	CN2	$[2s^22p_{1/2}(2p_{3/2})^2_2]_{5/2}$
LiBe7	$[2p_{1/2}2p_{3/2}]_2$	CN3	$[2s^22p_{1/2}(2p_{3/2})^2_0]_{1/2}$
LiBe8	$[2p^2_{3/2}]_2$	NO0	$[2s^2(2p_{1/2})^2(2p_{3/2})^2_2]_2$
BeB0	$[2s^22p_{1/2}]_{1/2}$	NO1	$[2s^2(2p_{1/2})^2(2p_{3/2})^2_0]_0$
BeB2	$[2s^22p_{3/2}]_{3/2}$	NO2	$[2s^22p_{1/2}(2p_{3/2})^3_{3/2}]_1$
BeB7	$[(2p_{1/2})^22p_{3/2}]_{3/2}$	NO3	$[2s^22p_{1/2}(2p_{3/2})^3_{3/2}]_2$
BeB11	$[2p_{1/2}(2p_{3/2})^2_2]_{3/2}$		

TABLE V. Calculated angular correction factors for the main *KLL* DR of He-like xenon ions.

	HeLi0	HeLi1	HeLi2
He1		1.00	1.00
He2	1.25		
He3	1.00		
He4	1.25		
He5	1.00		
He6	1.25		
He7			1.20
He8		1.25	0.80
He9			1.20
He10			0.80
He11			1.00

IV. RESULTS AND DISCUSSION

Fitting of the excitation functions found in experiments A and B led to the same electron beam energy spread, 42.8 eV at FWHM. With this energy spread, the DR of different charge states is mostly resolvable, although for some intermediate states, DR resonances of different charge states can be blended. However, the contributions from different charge states to the mixed resonances were not difficult to separate, as the resolvable DR resonances already defined the charge state distribution. By normalizing to the $n = 2$ RR differential cross sections, we obtained the *KLL* DR resonant strengths. The total *KLL* DR resonant strengths of He-like, Li-like, and up to O-like Xe ions are summarized in Table XI.

In this work, the uncertainties in determining the DR resonant strengths are around 9%. The admixture from different sources are as follows. First, statistic uncertainties are between 2% and 4% depending on the intensities of the resonant peaks. Second, the accuracy of RR cross-section calculations will influence the reliability for determining the DR strengths, as we obtained the latter by normalizing to the former. It is believed that this would introduce uncertainties no more than 3% [28,30,47] as calculations of RR are nowadays rather reliable. Third, in the data analysis, we obtained the charge states distribution by fitting the excitation functions using theoretical resonant strengths. The uncertainty in resonant strength calculations could transfer to the charge state distribution and, consequently, transfer to the final results. Following the method introduced in Ref. [27], we multiplied the theoretical resonant strengths randomly by 1.2 or 0.8 and then refitted the excitation functions to get a new charge state distribution. The results show an average deviation of 2.6% for the resonant strength. As an extreme case, we changed the theoretical resonant strengths randomly by 40% (that means randomly multiplied by 1.4 or 0.6); the resulting average deviation was 5.3%. From previous work [33], it was shown that the FAC calculation of the resonant strengths agreed with the experimental results within the experimental uncertainty, which was 20%. So we took the average deviation

TABLE VI. Calculated angular correction factors for the main *KLL* DR of Li-like xenon ions.

	LiBe0	LiBe1	LiBe2	LiBe3	LiBe4	LiBe5	LiBe6	LiBe7	LiBe8
Li1	0.76			0.76				0.98	
Li2		1.00	1.00						
Li3							1.18	0.83	0.83
Li4	0.78							0.98	
Li5					0.86				
Li6					1.17				
Li7		1.21	0.90		1.02	0.90			
Li8			1.13		0.87	1.13			
Li9		1.26	0.87			0.87			
Li10		1.24	0.88		1.02	0.88			
Li11			1.25		0.75	1.25			
Li12					1.17				
Li13					0.86	1.14			
Li14					1.00	1.00			
Li15					1.03	0.87			
Li16					0.76	1.24			

TABLE VII. Calculated angular correction factors for the main *KLL* DR of Be-like xenon ions.

	BeB0	BeB2	BeB7	BeB11	BeB12	BeB13
Be1	1.00					
Be2		1.20	1.20			
Be3	1.25	0.80				
Be4		1.20		1.20	0.77	
Be5		0.80			1.05	
Be6		1.00				1.00

of 2.6% for this uncertainty estimate. Fourth, ion abundancies change due to the DR resonances during the electron beam energy scanning, as already discussed in the last paragraph of the data analysis section. This will also introduce some uncertainties. Our estimation shows this would be at a level of 1.0%. The above four mentioned contributions are the main sources of error in our extracted data. Detailed numbers for the uncertainty in each resonant strength are listed in parenthesis in the table.

In Table XI, the experimental and theoretical results from this work and previous works [32,48–50] are listed. The two experimental results agree very well within the error bars. The present accuracy is significantly higher than that in the previous work [32]. Comparison of the experimental results with the calculations listed in Table XI shows that, except for the case of Li-like ions, all the calculations, including both present and previous works, are fully inside the experimental error bars. The agreement is excellent. In the Li-like case, the calculated resonant strength from the FAC code is smaller than the experimental results by about 14%. As there are no other calculations for Li-like Xe ions for comparison, we took the result of Li-like iodine by Shi *et al.* [51] for comparison. Iodine is next to xenon in the periodic table. Shi's work gave the total *KLL* DR resonant strength as 23.16 (10^{-20} cm^2 eV), which is very close to our calculation for Xe (23.74). This, in some sense, supports our calculation. As a further check, we calculated the DR resonant strength for Li-like I using the same FAC code and in the same way as we did for Xe. The result agrees with Shi's within 5%. In the FAC code, the Breit interaction was not included in autoionization rate calculations. However, in Shi's work, the Breit interaction was included. The agreement between the two calculation implies that the Breit interaction does not affect the total resonant strength in a pronounced way, at least in this case. So the deviation between the experimental and theoretical results in the Li-like case must have other causes. One fact which is possibly worth noticing is that Shi's result for Li-like I is 20% smaller than the experimental result by Watanabe *et al.* [31]. This situation is similar to that encountered here, and the reason is not known at the present time. We call on further theoretical and experimental works for Li-like ions in this range of atomic numbers.

Figure 6 shows the experimental and theoretical results of the *KLL* DR strengths of the ions in the He iso-electronic sequence. The experimental results are Ar^{16+} by Ali *et al.* [20] and Zou *et al.* [22], Ti^{20+} by O'Rourke *et al.* [26], Fe^{24+} by Beiersdorfer *et al.* [24], Ni^{26+} by Knapp *et al.* [27], Ni^{26+}, Mo^{40+}, and Ba^{54+} by Knapp *et al.* [28], Ge^{30+} by Zhang *et al.* [25], I^{51+} by Watanabe *et al.* [31], and Xe^{52+} from this work. The theoretical results are from the present FAC calculation.

TABLE VIII. Calculated angular correction factors for the main *KLL* DR of B-like xenon ions.

	BC0	BC1	BC2	BC5	BC6
B1		1.18	0.82		
B2	1.25	0.88	1.03		
B3		1.19	0.81	0.81	
B4			1.17	1.17	
B5		0.87	1.03	1.03	
B6		1.18	0.82	0.82	
B7		1.00	1.00		1.00
B8		1.00			

The calculations agree with most of the experimental resonant strengths, with only two exceptions. One is the result of Ni^{26+} by Knapp *et al.* [28] done in 1993. The calculation in that work already showed disagreement with the experiment for Ni^{26+} but agrees with our present calculation. On the other hand, their previous experimental result [27] four years earlier shows excellent agreement with the present calculation. The second discrepancy is for I^{51+} [31]. Here the experimental result is significantly higher (about 18%) than the present calculation. But Shi's calculation [51] for I^{51+} shows perfect agreement with our FAC result. Different from the previously mentioned Li-like case, our He-like Xe DR strength agrees with theoretical results. So further work on He-like I is also requested.

With the data analysis procedure described earlier, we could also resolve DR processes for several intermediate states in He-, Li-, Be-, B-, and C-like ions and obtained state resolved DR strengths. For those DR processes with very close resonant energies, which could not be resolved, we attempted to obtain summed resonant strengths. In Table XII, we list the state resolved and summed *KLL* DR resonant strengths of He- to O-like Xe ions measured and calculated in this work. Also shown are the available theoretical results from previous works [48–50]. In the He-like case, the *KLL* DR from the ground state through the intermediate states of $[1s2s^2]_{1/2}$, $[(1s2s)_0 2p_{1/2}]_{1/2}$, and $[1s(2p_{3/2})^2_2]_{5/2}$ were resolved, and the strengths were obtained. The two different calculations for He-like ions agree very well with each other and agree with our experiment within the experimental uncertainties for the intermediate states of, $[1s2s^2]_{1/2}$ and $[1s(2p_{3/2})^2_2]_{5/2}$, but slightly outside the error bar for $[(1s2s)_0 2p_{1/2}]_{1/2}$. All the experimental results for B-, C-, N-, and O-like Xe and some of the results for Be-like

TABLE IX. Calculated angular correction factors for the main *KLL* DR of C-like xenon ions.

	CN0	CN1	CN2	CN3
C1	1.20	1.20	0.77	
C2	0.80	0.80	1.05	
C3	1.00			1.00

TABLE X. Calculated angular correction factors for the main *KLL* DR of N-like xenon ions.

	NO0	NO1	NO2	NO3
N1	0.98		1.02	0.98
N2	1.00	1.03	0.98	1.00

Xe ions agree very well with the listed theoretical results. One of the obtained DR resonance strengths for Be-like Xe, which is a summation over the the mixed intermediate states, $[1s2s^2(2p_{3/2})_2^2]_{3/2}$ and $[1s2s^2(2p_{3/2})_0^2]_{1/2}$, is larger by 16% compared with the present FAC calculation result. Also the FAC result is higher than the previous calculation [49] by a further 16%. The worst agreement between the experimental and theoretical resonant strength is seen in the Li-like case. Among the seven resonant strengths obtained for this charge state, three of them agree with the FAC calculation within the experimental uncertainties, which are around 9%. The other four are all larger than the FAC results by at least 16%. In the worst case, they are 44% larger than the calculation, which is for the intermediate state of $[1s2s^22p_{1/2}]_1$. One of the possible causes of this large discrepancy could be from leaving out the Breit interaction in the calculation of autoionization rates using the FAC code. For the intermediate state of $[1s2s^22p_{1/2}]_1$, a large influence from the Breit interaction was found in the works of [29,52], and a distortion of the angular distribution of about 10% was shown at 90° for the iodine ions. We would expect that for Xe ions, the distortion for the same resonance would be about the same. More theroretical work is needed before any conclusion can be made regarding the reason for the previously mentioned discrepancy and the effects of the Breit interaction.

In the data analysis in this work, the angular correction factors were all calculated by using the FAC code, which means the Breit interaction was not included in the autoionization part. This could possibly introduce some more uncertainties in determining the resonant strengths (but not likely to be more than 10%). As we cannot estimate how much it contributes to the uncertainties, we disregarded it in the uncertainty analysis.

TABLE XI. The total *KLL* DR resonant strength (10^{-20} cm^{2}eV) of He-like to O-like Xe ions. Uncertainties are listed in parentheses.

	Experiment		Theory	
Ion	Present	Others	Present	Others
He-like	31.42(3.02)		33.54	32.87[b]
Li-like	27.51(2.56)		23.74	
Be-like	19.79(1.78)	19.22(3.54)[a]	19.50	18.63[c]
B-like	11.93(1.06)		12.09	12.00[d]
C-like	6.22(0.57)	6.52(1.27)[a]	5.74	
N-like	2.48(0.23)		2.60	
O-like	0.86(0.08)		0.81	

[a]Reference [32].
[b]Reference [48].
[c]Reference [49].
[d]Reference [50].

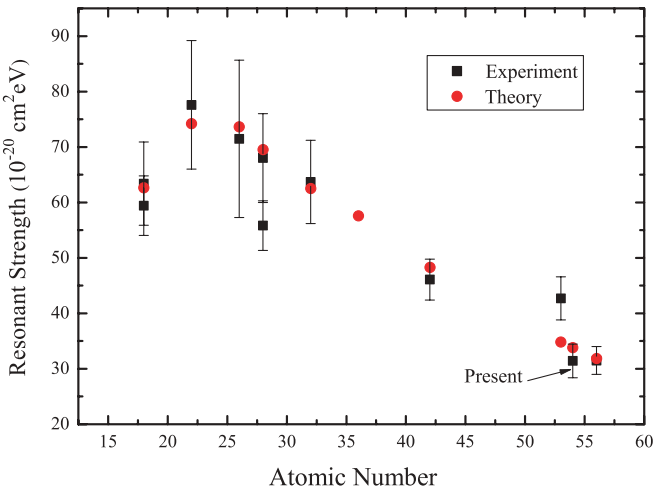

FIG. 6. (Color online) The *KLL* resonance strengths of He-like ions. The other experimental results are Ar^{16+} by Ali *et al.* [20] and Zou *et al.* [22], Ti^{20+} by O'Rourke *et al.* [26], Fe^{24+} by Beiersdorfer *et al.* [24], Ni^{26+} by Knapp *et al.* [27], Ni^{26+}, Mo^{40+}, and Ba^{54+} by Knapp *et al.* [28], Ge^{30+} by Zhang *et al.* [25], and I^{51+} by Watanabe *et al.* [31]. The theoretical results are from this work.

Instead we listed all the angular correction factors used in this work, in Tables V–X. In the future, when more precise angular correction factors become available, better resonant strengths can be derived by normalizing the present resonant strengths to the ratios of the present over future angular correction factors, for the resolvable resonances.

TABLE XII. The state resolved and unresolved *KLL* DR resonant strength (10^{-20} cm^2 eV) of He-like to O-like Xe ions measured and calculated in this work, together with some available theoretical results from references. Uncertainties are listed in parentheses.

Ion	State	Expt.	Theor.	Ref.
He-like	He1	2.72(0.26)	2.57	2.59[a]
	He3	3.70(0.36)	3.24	3.27[a]
	He9	4.25(0.41)	4.35	4.48[a]
Li-like	Li1	2.56(0.24)	1.43	
	Li2	0.43(0.04)	0.41	
	Li4+Li5+Li6	4.57(0.43)	4.38	
	Li7+Li8+Li9	5.83(0.54)	5.74	
	Li10+Li11	3.98(0.37)	3.31	
	Li13+Li14	2.66(0.25)	2.19	
	Li15+Li16	2.91(0.27)	2.08	
Be-like	Be2+Be3	11.43(1.03)	11.64	10.87[b]
	Be4	3.61(0.32)	3.59	3.86[b]
	Be5+Be6	3.81(0.34)	3.20	2.69[b]
B-like	B3+B4+B5	4.05(0.36)	4.14	4.37[c]
	B6+B7+B8	2.27(0.20)	2.22	2.02[c]
C-like	C1	3.26(0.30)	2.96	
	C2+C3	2.96(0.27)	2.76	
N-like	N1+N2	2.46(0.23)	2.60	
O-like	O1	0.86(0.08)	0.81	

[a]Reference [48].
[b]Reference [49].
[c]Reference [50].

For heavier elements, the Breit interaction will be more pronounced. Hence, to get reliable experimental DR resonant strengths, systematic calculations including the Breit interaction for the angular distribution of the DR stabilization radiation are highly required.

V. CONCLUSIONS

In this work, *KLL* DR resonant strengths of He-like to O-like Xe ions were studied. For the total resonant strengths, the present experimental and theoretical results of He-, Be-, B-, C-, N-, and O-like agree very well. But the DR results for Li-like Xe have some problems. The theoretical result is 14% smaller than the experimental. Similar problems are seen in the comparison of theoretical [51] and experimental [31] results for I^{51+}. The theoretical strength [51] is about 20% smaller than the experiment [31] in that case. Comparing the available experimental results with our present calculation on the total resonant strengths along the He electronic sequence shows there is a discrepancy for I^{51+}. The experimental strength [31] is 18% higher then the present calculation and 20% higher than the previous calculation [51]. The present FAC calculation of the total DR strengths was compared with the other available calculations. They agree with each other irrespective of whether the Breit interaction was included in the autoionization rate calculation. This means the Breit interaction does not affect the total resonant strength in a pronounced way in the systems considered in the present work.

As a conclusion, further *KLL* DR studies, both experimental and theoretical, are required for Li-like and He-like ions around the atomic numbers of 53 and 54. In particular, studies for Li-like ions are needed to solve the mystery of the underprediction of the total *KLL* DR strength.

ACKNOWLEDGMENTS

This work was supported by the National Natural Science Foundation of China under Grant No. 10434050, Chinese National Fusion Project for ITER No. 2009GB106001, and Shanghai Leading Academic Discipline Project No. B107.

[1] A. Burgess, Astrophys. J. **139**, 776 (1964).
[2] J. Dubau and S. Volonte, Rep. Prog. Phys. **43**, 199 (1980).
[3] D. S. Belic, G. H. Dunn, T. J. Morgan, D. W. Mueller, and C. Timmer, Phys. Rev. Lett. **50**, 339 (1983).
[4] TFRGroup, F. Bombarda, F. Bely-Dubau, P. Faucher, M. Cornille, J. Dubau, and M. Loulergue, Phys. Rev. A **32**, 2374 (1985).
[5] M. Bitter, H. Hsuan, K. W. Hill, and M. Zarnstorff, Phys. Scr. **T47**, 87 (1993).
[6] P. Beiersdorfer, A. L. Osterheld, T. W. Phillips, M. Bitter, K. W. Hill, and S. von Goeler, Phys. Rev. E **52**, 1980 (1995).
[7] R. Radtke, C. Biedermann, T. Fuchs, G. Fußmann, and P. Beiersdorfer, Phys. Rev. E **61**, 1966 (2000).
[8] C. Biedermann, R. Radtke, and K. B. Fournier, Phys. Rev. E **66**, 066404 (2002).
[9] H. S. W. Massey and D. R. Bates, Rep. Prog. Phys. **9**, 62 (1942).
[10] G. Kilgus *et al.*, Phys. Rev. Lett. **64**, 737 (1990).
[11] W. Spies *et al.*, Phys. Rev. Lett. **69**, 2768 (1992).
[12] D. R. DeWitt, R. Schuch, H. Gao, W. Zong, S. Asp, C. Biedermann, M. H. Chen, and N. R. Badnell, Phys. Rev. A **53**, 2327 (1996).
[13] D. W. Savin *et al.*, Astrophys. J. **576**, 1098 (2002).
[14] T. Mohamed, D. Nikolić, E. Lindroth, S. Madzunkov, M. Fogle, M. Tokman, and R. Schuch, Phys. Rev. A **66**, 022719 (2002).
[15] D. W. Savin *et al.*, Astrophys. J. **642**, 1275 (2006).
[16] D. V. Lukić *et al.*, Astrophys. J. **664**, 1244 (2007).
[17] E. W. Schmidt *et al.*, Phys. Rev. A **76**, 032717 (2007).
[18] C. Brandau *et al.*, Int. J. Radiat. Phys. Chem. **75**, 1763 (2006).
[19] R. Ali, C. P. Bhalla, C. L. Cocke, and M. Stockli, Phys. Rev. Lett. **64**, 633 (1990).
[20] R. Ali, C. P. Bhalla, C. L. Cocke, M. Schulz, and M. Stockli, Phys. Rev. A **44**, 223 (1991).
[21] A. J. Smith, P. Beiersdorfer, K. Widmann, M. H. Chen, and J. H. Schofield, Phys. Rev. A **62**, 052717 (2000).
[22] Y. Zou, J. R. Crespo López-Urrutia, and J. Ullrich, Phys. Rev. A **67**, 042703 (2003).
[23] H. Watanabe, F. J. Currell, H. Kuramoto, Y. M. Li, S. Ohtani, B. O'Rurke, and X. M. Tong, J. Phys. B **34**, 5095 (2001).
[24] P. Beiersdorfer, T. W. Phillips, K. L. Wong, R. E. Marrs, and D. A. Vogel, Phys. Rev. A **46**, 3812 (1992).
[25] X. Zhang, J. R. C. López-Urrutia, P. Guo, V. Mironov, X. Shi, A. J. G. Martínez, H. Tawara, and J. Ullrich, J. Phys. B **37**, 2277 (2004).
[26] B. E. O'Rourke, H. Kuramoto, Y. M. Li, S. Ohtani, X. M. Tong, H. Watanabe, and F. J. Currell, J. Phys. B **37**, 2343 (2004).
[27] D. A. Knapp, R. E. Marrs, M. A. Levine, C. L. Bennett, M. H. Chen, J. R. Henderson, M. B. Schneider, and J. H. Scofield, Phys. Rev. Lett. **62**, 2104 (1989).
[28] D. A. Knapp, R. E. Marrs, M. B. Schneider, M. H. Chen, M. A. Levine, and P. Lee, Phys. Rev. A **47**, 2039 (1993).
[29] N. Nakamura, A. P. Kavanagh, H. Watanabe, H. A. Sakaue, Y. Li, D. Kato, F. J. Currell, and S. Ohtani, Phys. Rev. Lett. **100**, 073203 (2008).
[30] T. Fuchs, C. Biedermann, R. Radtke, E. Behar, and R. Doron, Phys. Rev. A **58**, 4518 (1998).
[31] H. Watanabe, H. Tobiyama, A. P. Kavanagh, Y. M. Li, N. Nakamura, H. A. Sakaue, F. J. Currell, and S. Ohtani, Phys. Rev. A **75**, 012702 (2007).
[32] W. D. Chen *et al.*, Phys. Plasmas **14**, 103302 (2007).
[33] W. D. Chen, J. Xiao, Y. Shen, Y. Q. Fu, F. C. Meng, C. Y. Chen, B. H. Zhang, Y. J. Tang, R. Hutton, and Y. Zou, Phys. Plasmas **15**, 083301 (2008).
[34] D. R. DeWitt, D. Schneider, M. W. Clark, M. H. Chen, and D. Church, Phys. Rev. A **44**, 7185 (1991).
[35] D. R. DeWitt, D. Schneider, M. H. Chen, M. B. Schneider, D. Church, G. Weinberg, and M. Sakurai, Phys. Rev. A **47**, R1597 (1993).

[36] D. R. DeWitt, D. Schneider, M. H. Chen, M. W. Clark, J. W. McDonald, and M. B. Schneider, Phys. Rev. Lett. **68**, 1694 (1992).
[37] M. B. Schneider, D. A. Knapp, M. H. Chen, J. H. Scofield, P. Beiersdorfer, C. L. Bennett, J. R. Henderson, R. E. Marrs, and M. A. Levine, Phys. Rev. A **45**, R1291 (1992).
[38] W. D. Chen, J. Xiao, Y. Shen, Y. Q. Fu, F. C. Meng, C. Y. Chen, Y. Zou, and R. Hutton, Rev. Sci. Instrum. **79**, 123304 (2008).
[39] X. Zhu *et al.*, Nucl. Instrum. Methods B **235**, 509 (2005).
[40] W. Hu *et al.*, Can. J. Phys. **86**, 321 (2008).
[41] M. Tokman *et al.*, Phys. Rev. A **66**, 012703 (2002).
[42] J. R. Henderson *et al.*, Phys. Rev. Lett. **65**, 705 (1990).
[43] P. Beiersdorfer *et al.*, Phys. Rev. A **53**, 3974 (1996).
[44] P. Beiersdorfer, G. Brown, S. Utter, P. Neill, K. J. Reed, A. J. Smith, and R. S. Thoe, Phys. Rev. A **60**, 4156 (1999).
[45] A. S. Shlyaptseva, R. C. Mancini, P. Neill, P. Beiersdorfer, J. R. Crespo López-Urrutia, and K. Widmann, Phys. Rev. A **57**, 888 (1998).
[46] A. S. Shlyaptseva, R. C. Mancini, P. Neill, and P. Beiersdorfer, J. Phys. B **32**, 1041 (1999).
[47] M. F. Gu, Astrophys. J. **589**, 1085 (2003).
[48] J. Nilsen, At. Data Nucl. Data Tables **38**, 339 (1988).
[49] M. H. Chen, At. Data Nucl. Data Tables **38**, 381 (1988).
[50] M. H. Chen, K. J. Reed, and D. M. McWilliams, At. Data Nucl. Data Tables **65**, 289 (1997).
[51] Y. Shi, C. Dong, and D. Zhang, Phys. Lett. **A372**, 4913 (2008).
[52] S. Fritzsche, A. Surzhykov, and T. Stohlker, Phys. Rev. Lett. **103**, 113001 (2009).